

# ATLAS jet trigger system - overview and performance at the beginning of Run 3

---

Ondřej Theiner<sup>a,\*</sup> on behalf of the ATLAS Collaboration

<sup>a</sup>*Université de Genève,  
Rue de l'Ecole-De-Médecine 20, 1205 Genève, Switzerland*  
E-mail: [ondrej.theiner@cern.ch](mailto:ondrej.theiner@cern.ch)

As a hadron collider, the LHC produces a large number of hadronic jets. Properties of these jets are good tests of QCD and they are produced in both Standard Model processes and beyond the Standard Model scenarios. The ATLAS jet trigger system is an important element of the event selection process, providing data to study a wide range of physics processes at the LHC. To this end, proper jet reconstruction and calibration are crucial to ensure good trigger performance across the ATLAS physics program, and understanding this performance is necessary for the correct interpretation of recorded data. In this contribution, we provide an overview of the ATLAS jet trigger system and its general performance at the beginning of Run 3 at the LHC.

ICHEP 2024  
18-24 July 2024  
Prague, Czech Republic

---

\*Speaker



## 1. Introduction

Proton bunch crossings at the LHC are happening at approximately 40 MHz, and the average size of a single event is 2.5 MB. If every event were recorded, we would get 1 PB of data in 10 s of data-taking. Such a large volume of data would be nearly impossible to store and process. Moreover, the data acquisition system bandwidth would not allow the transfer of such a large amount of data. Therefore the *Trigger and Data Acquisition System* (TDAQ) is crucial for properly working detector, recording only potentially interesting events.

The ATLAS TDAQ system is divided into two levels: *Level-1* (L1) and the *High-Level Trigger* (HLT). The L1 system is hardware-based, and it has to decide whether the event will be stored or discarded within  $2.5 \mu\text{s}$ , and it reduces the incoming rate of 40 MHz down to 100 kHz. Since the decision has to be made quickly, only partial information about the event is available. This decision is made based on the information about muons, electrons, photons, jets, and large missing transverse momentum ( $E_{\text{T}}^{\text{miss}}$ ).

Once the event has passed through the L1 trigger, it is evaluated by the software-based HLT, which has to decide on average in 0.5 s. More sophisticated algorithms than the L1 trigger can run at this level, thanks to the longer latency. It reduces the trigger rate from 100 kHz down to 3 kHz.

Since jets are one of the most common signatures at the LHC and are often connected to interesting Standard Model (SM) processes and processes sensitive to new physics, jet triggers are one of the pivotal triggers for ATLAS.

The following sections present the overview of the ATLAS jet trigger system at the beginning of Run 3.

## 2. Jet trigger at Level-1

The jet trigger system at L1 is based on the information from the calorimeter, and it has undergone several upgrades since Run 2. The ATLAS L1 trigger at Run 3 uses finer granularity of the calorimeter, and it works with the information from *Super Cells* [5], which is the finer segmentation of calorimeter towers used in Run 1 and 2. The information is processed by *Feature Extractor* (FEX) processor [7], which is divided into three subsystems: electromagnetic (eFEX), jet (jFEX), and global (gFEX) feature extractors. jFEX and gFEX are used for the jet triggers.

jFEX can reconstruct small- $R$  jets using the sliding window algorithm, and its performance is similar to the L1Calo system from Run 2 for single jets. However, the improvement comes in the case of multi-jet triggers due to the better resolution of close-by jets. gFEX, on the contrary, uses coarser granularity than jFEX, which is used to reconstruct large- $R$  jets. The single jet trigger efficiencies for the small- $R$  jet triggers using jFEX are shown in figure 1(a). These can be compared with the trigger efficiencies of the legacy L1 single jet triggers in figure 1(b).

## 3. Jet trigger at the HLT

The HLT can run more complicated algorithms compared to the L1 system, and, in Run 3, it uses *Particle Flow* reconstruction [6]. This approach combines the information from the calorimeter and the tracker. In this process, tracks are matched to clusters where they created energy deposits; the

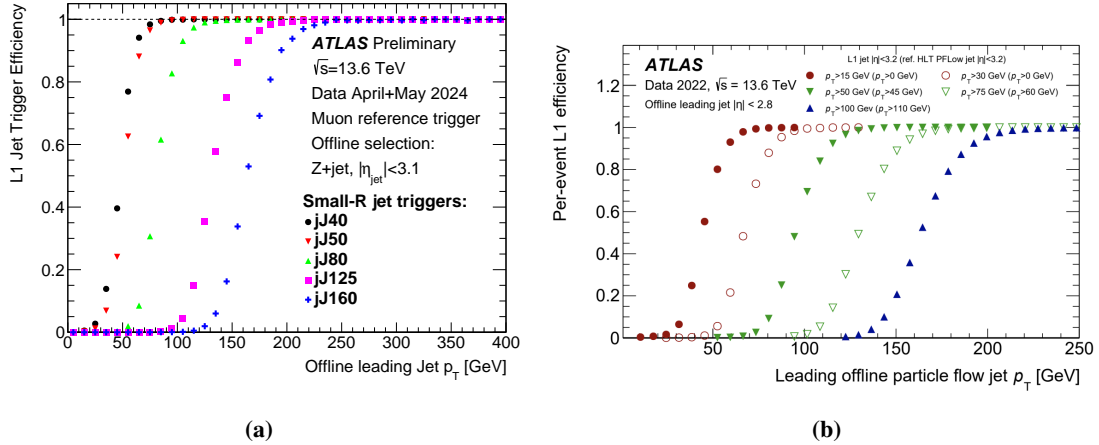


**Figure 1:** (a) L1Calo single jet trigger efficiencies for the Phase-I system in Run 3. The number in the trigger name represents the approximate 50 % efficiency point at the offline jet scale [1]. (b) Efficiency of the legacy L1 single jet triggers. [2]

amount of deposited energy is estimated based on the track momentum, which must be subtracted from the calorimeter measurement to avoid double-counting. The track reconstruction uses the full scan tracking, similar to the reconstruction offline. This is possible thanks to the calorimeter-only jet selections (*calorimeter preselections*) based on the topo-cluster jets allowing to bridge the large gap between Level-1 and HLT thresholds. After the process of track-to-cluster matching and energy removal, as mentioned before, the resulting Particle Flow Objects (PFOs) are used as inputs for the anti- $k_t$  jet reconstruction algorithm. The output, commonly referred to as PFlow jets, is used in the HLT decisions<sup>1</sup>.

Before the trigger decision is made, jets are calibrated using the calibration procedure to match reconstructed jets to those reconstructed offline as closely as possible. The jet calibrations are discussed in the next section. Figure 2(a) shows the single jet HLT efficiency, and figure 2(b) shows the multi-jet HLT trigger efficiency for jets in the pseudorapidity region  $|\eta| < 3.2$ .

### 3.1 Jet calibrations

The response of the jet with different  $p_T$  reconstructed at the HLT level differs from the offline jets at the electromagnetic scale. These effects must be accounted for, and the calibration procedure is introduced. The calibration process is also done in the offline reconstruction to correct for the non-compensating calorimeter effects, pile-up, or the fact that the primary collision vertex is not precisely at the center of the detector. The online calibration follows a similar procedure, and the goal is to achieve a jet response similar to offline reconstruction; in other words, the ratio of HLT/offline response has to be close to 1.

This response differs for different transverse momenta, so it is studied for different  $p_T$  slices. The mean and  $1\sigma$  quantile of the distribution HLT/offline are estimated for each slice, see figure 3(a). This figure shows the HLT jet calibration performance for the year 2023. However, at the beginning of Run 3, there was not enough data to derive calibration factors between offline and

<sup>1</sup>The system in the Run 2 was using information only from the calorimeter topo-clusters.

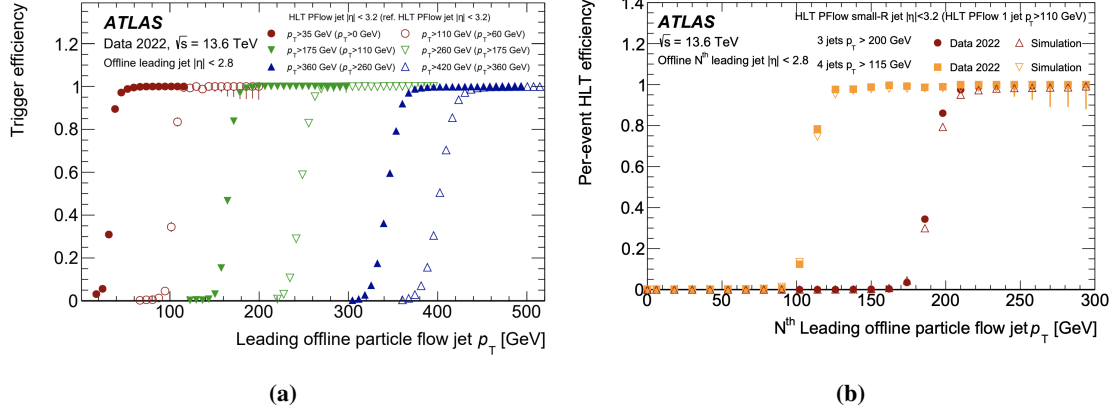


**Figure 2:** (a) Single jet HLT efficiencies for jets in the central region. [2]. (b) Multi-jet trigger efficiency at the HLT. [2]

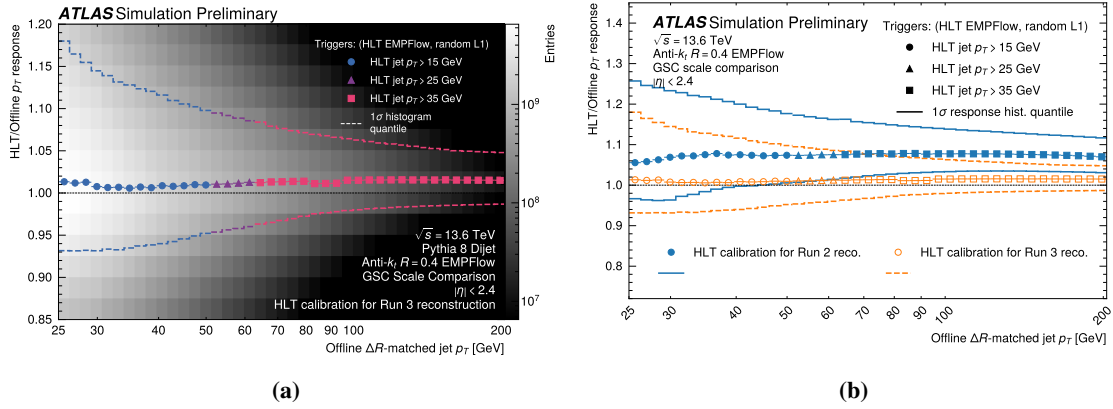


**Figure 3:** (a) HLT jet calibration performance for 2023 [1]. (b) Comparison between HLT jet calibration using Run 2 (blue) and Run 3 (orange) reconstruction [1].

online reconstructions, and this is why the offline reconstruction used Run 3 calibration, while the HLT used Run 2 calibration. This disagreement caused inefficiency in the jet calibration, and the jet response was lower than in 2023. A comparison of the two calibrations can be seen in figure 3(b), where the orange color represents the plot shown in figure 3(a).

### 3.2 $b$ -jet trigger

$b$ -jet triggers are crucial for the precision measurements and searches, which is why identifying events containing  $b$ -jet -  $b$ -tagging is essential. Processes with  $b$ -jet in the final state are interesting for SM Higgs physics ( $H \rightarrow b\bar{b}$ ,  $HH \rightarrow b\bar{b}b\bar{b}$ ), top physics  $t \rightarrow Wb$ , beyond SM searches, or they can be used as a veto for many backgrounds. The identification of  $b$ -jets is based on the relatively long lifetime of  $b$ -hadrons, which allows them to travel several millimeters from the primary interaction vertex before they decay. This property is the critical element of  $b$ -tagging, which is why the  $b$ -tagging requires precise tracking.

The  $b$ -jet identification at the HLT is done in two steps. The first fast  $b$ -tagging [8] is executed

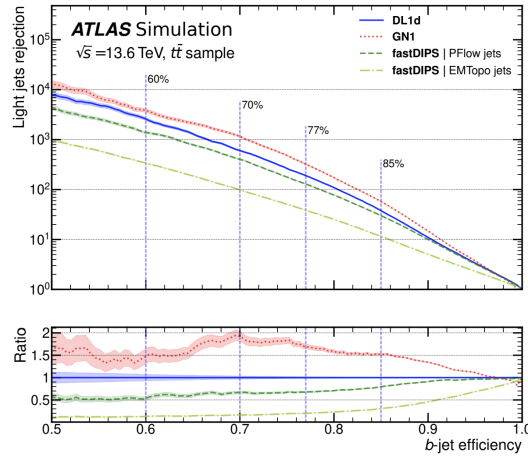


**Figure 4:** Light jets rejection by different  $b$ -tagging algorithms [2].

on tracks inside the *super-Region-of-Interest* [9], which is the region of the detector selected by the L1 trigger, where the potentially interesting physics can be happening, and it employs the fast  $b$ -tagging algorithm. The *fastDIPS* algorithm using the *Deep Sets* [3] based neural network was used for the fast  $b$ -tagging at the beginning of the Run 3 and was replaced by the graph neural network *fastGN2*.

The second stage of  $b$ -tagging is running one of the higher-level algorithms based on neural networks. Thanks to the fast progress in the field of machine learning, the HLT in Run 3 was using deep neural network *DL1d* at the beginning, which was later replaced by graph neural network *GN1*, which was replaced by another graph neural network *GN2*. The comparison of the performance of higher level  $b$ -tagging algorithms used in Run 3 is shown in figure 4, where the rejection of light jets and  $c$ -jets is compared for all three algorithms.

## 4. Conclusion

An efficient jet trigger system is crucial for targeting many interesting SM and beyond SM processes, and is achieved thanks to the optimized trigger system, which underwent several improvements before and at the beginning of Run 3.

The major improvement at the L1 is the use of FEX, which allows object identification at the low level of the hardware electronics. This system allows for better triggering performance and employs efficient multi-jet triggers.

The jet trigger performance of the HLT was significantly improved compared to previous runs in several aspects. These improvements include the implementation of Particle Flow object reconstruction, enabled by enhanced tracking capabilities, calorimeter-based preselection stage to reduce CPU costs, and advancements in trigger-level jet calibration. Additionally,  $b$ -tagging preselections utilizing *fastDIPS* and *fastGN2* contributed to more efficient  $b$ -tagging triggers, while the use of graph neural networks *GN1* and *GN2* further enhanced  $b$ -tagging performance. It promises to enable crucial Standard Model measurements and powerful searches for new physics.

## References

- [1] ATLAS Collaboration *Public Jet Trigger Plots for Collision Data*, <https://twiki.cern.ch/twiki/bin/view/AtlasPublic/JetTriggerPublicResults>
- [2] ATLAS Collaboration *The ATLAS Trigger System for LHC Run 3 and Trigger performance in 2022*, *Journal of Instrumentation* **19** P06029 <https://doi.org/10.48550/arXiv.2401.06630>
- [3] ATLAS Collaboration *Deep Sets based Neural Networks for Impact Parameter Flavour Tagging in ATLAS*, ATL-PHYS-PUB-2020-014 (2020), <https://cds.cern.ch/record/2718948>
- [4] ATLAS Collaboration *Jet Flavour Tagging With GN1 and DL1d. Generator dependence, Run 2 and Run 3 data agreement studies*, <https://atlas.web.cern.ch/Atlas/GROUPS/PHYSICS/PLOTS/FTAG-2023-01/>
- [5] The Phase-I trigger readout electronics upgrade of the ATLAS Liquid Argon calorimeters <https://iopscience.iop.org/article/10.1088/1748-0221/17/05/P05024>
- [6] Aaboud, M., Aad, G., Abbott, B. et al. Jet reconstruction and performance using particle flow with the ATLAS Detector. *Eur. Phys. J. C* **77**, 466 (2017) <https://doi.org/10.1140/epjc/s10052-017-5031-2>
- [7] Technical Design Report for the Phase-I Upgrade of the ATLAS TDAQ System <https://cds.cern.ch/record/1602235>
- [8] Aad, G., Abbott, B. et al. Fast b-tagging at the high-level trigger of the ATLAS experiment in LHC Run 3. *Journal of Instrumentation* **18** P11006 <https://iopscience.iop.org/article/10.1088/1748-0221/18/11/P11006>
- [9] ATLAS Collaboration., Aad, G., Abbott, B. et al. Configuration and performance of the ATLAS b-jet triggers in Run 2. *Eur. Phys. J. C* **81**, 1087 (2021) <https://doi.org/10.1140/epjc/s10052-021-09775-5>